



1    **Hydrological processes and permafrost regulate magnitude, source**  
2    **and chemical characteristics of dissolved organic carbon export in a**  
3    **peatland catchment of northeastern China**

4

5    Yuedong Guo<sup>1</sup>, Changchun Song<sup>1,\*</sup>, Wenwen Tan<sup>1</sup>, Xianwei Wang<sup>1</sup>, Yongzheng Lu<sup>1</sup>

6    <sup>1</sup>Key Laboratory of Wetland Ecology and Environment, Northeast Institute of  
7    Geography and Agroecology, Chinese Academy of Sciences, Changchun 130012,  
8    China

9    Tel: 86-431-85542211

10    Fax: 86-431-85542298

11    Address:

12        Northeast institute of Geography and Agroecology, Chinese Academy of Sciences.  
13    No.4888, Shengbei Road, Changchun, Jilin Province, China, 086-130102

14

15    **Abstract**

16        Permafrost thawing in peatland has the potential to alter the catchment  
17    export of dissolved organic carbon (DOC), thus influencing carbon  
18    cycling in linked aquatic and ocean ecosystems. However, peatland along  
19    the southern margins of Eurasian permafrost are seldom examined in  
20    spite of the presence of considerable risks associated with degradation  
21    due to climate warming. This study examines dynamics of DOC export  
22    from a permafrost peatland catchment located in northeastern China



23 during the growing seasons of 2012 to 2014. Our findings show that  
24 runoff processes affect observed DOC concentrations, magnitudes,  
25 sources, and chemical characteristics of stream discharge. The entire  
26 catchment exhibits strong potential for annual DOC exporting ( $4.87 \text{ g C}$   
27  $\text{m}^{-2}$ ), and DOC from the peatland landscape alone is estimated to amount  
28 to  $12.89 \text{ g C m}^{-2}$ . Annual DOC export processes are closely related to  
29 total discharge levels, and floods contribute to approximately 85% of  
30 DOC export levels. Flood volumes derived mainly from peat pore water  
31 stored in the upper organic layer of the soil profile prior to rainfall events,  
32 creating a strong linkage between discharge and DOC concentrations.  
33 DOC source and chemical characteristics, as indicated by three  
34 fluorescence indexes, have changed regularly according to source shifts  
35 occurring as a result of flood and baseflow processes. A deepening of the  
36 active layer due to climate warming should elevate proportions of  
37 microbial-originated DOC in the baseflow. Given expected future  
38 increases in precipitation, our results show that the magnitude of DOC  
39 exports from the study region will increase.

40

## 41 **1. Introduction**

42 Permafrost soils have acted as sinks for atmospheric carbon (C) since  
43 at least the late Pleistocene and serve as key sources of dissolved organic  
44 carbon (DOC) for linked aquatic and ocean ecosystems (Opsahl et al.,



45 1999; Kicklighter et al., 2013). As changes in the quantity and quality of  
46 exported DOC could greatly alter the energy cycles of linked oceans,  
47 considerable advances have been made in recent years to better evaluate  
48 potential changes DOC export patterns from permafrost regions  
49 (Townsend-Small et al., 2011; Vonk et al., 2013;). However,  
50 uncertainties remain regarding to main driving factors involved and the  
51 fate of DOC due to complex interactions between hydrological and  
52 thermal dynamics and bio-chemical drivers (Olefeldt and Roulet, 2012;  
53 Kicklighter et al., 2013).

54 Significant losses of near-surface permafrost have been observed over  
55 the past century and such outcomes have induced considerable changes in  
56 hydrological processes and soil thermal regimes (Lyon et al., 2009;  
57 Lessels et al., 2015), in turn altering the magnitude and timing of  
58 terrestrial DOC export processes. Hydrological processes are an  
59 important and well-documented regulator of DOC export from permafrost  
60 regions (Ågren et al., 2010; Guo et al., 2015). Owing to increased levels  
61 of hydrological access to previously frozen soils following permafrost  
62 degradation, DOC export is forecasted to increase in Siberian rivers along  
63 a latitudinal transect (Frey and MacClelland, 2009). However, permafrost  
64 degradation also increases the likelihood of interactions occurring  
65 between subsurface flows and mineral soils, which in turn lead to  
66 considerable levels of DOC absorption by fine soil particles and which



67 decrease levels of DOC export magnitude (Petroni et al., 2006; Striegl et  
68 al., 2007). There are significant disparities in DOC export concentrations  
69 and seasonal patterns between surface- and subsurface-dominated runoff  
70 processes in permafrost catchments (Laudon et al., 2011). Studies have  
71 proven that capacities for DOC export from permafrost soils are closely  
72 related to lateral subsurface flows (Striegl et al., 2007; Lyon et al., 2010).  
73 Therefore, alterations in hydrological pathways during permafrost  
74 freeze-thaw cycles are some of the most important factors to consider in  
75 evaluating DOC export potential.

76 Hydrological pathways control not only on the availability of DOC  
77 produced along the surfaces of soil particles but also hydrological  
78 connectivity at the landscape scale, which determines physical transport  
79 routes of DOC release from a catchment (Birkel et al., 2014). A strong  
80 hydrological connection generally contributes to high levels of DOC  
81 export magnitude (Olfeldt and Roulet, 2012; Lessels et al., 2015). A  
82 catchment with 4% peatland cover achieve a 12% higher level of annual  
83 DOC export than an upland catchment due to maintained levels of  
84 hydrological connectivity (Olfeldt and Roulet, 2014). However,  
85 uncertainties remain in predicting DOC export processes based on  
86 changing hydrological processes. Levels of annual DOC export from  
87 permafrost are known to vary greatly between different landscapes and  
88 regions, e.g., at rates of between 1 and 35 g C m<sup>-1</sup> yr<sup>-1</sup> (Fraser et al., 2001;



89 Dinsmore et al., 2010), where variations mainly relate to hydrological  
90 regimes (Holden, 2005).

91 Flow pathways also determine chemical compositions of DOC  
92 export from permafrost catchments, which in turn have considerable  
93 impacts on downstream DOC mineralization levels and on C emissions  
94 from streams, lakes and oceans (Mann et al., 2012; Cory et al., 2014).  
95 Runoff processes can alter export compositions to a certain degree  
96 according to pathways of the organic-mineral soil layer. Mineral soil  
97 particles can stably absorb dissolved organic matter high in aromatic  
98 components with large molecular weights or acidic functional groups  
99 (Kalbitz et al., 2005) as well as aromatic structures while hydrophilic  
100 fatty microbial products with low molecular weights are desorbed and  
101 released (Striegl et al., 2005). To date, no satisfactory theoretical  
102 framework or method has been developed to quantify alterations in DOC  
103 chemical characteristics following permafrost degradation. More detailed  
104 surveys on comprehensive effects of hydrological processes are still  
105 needed to predict alterations in the magnitudes and chemical  
106 characteristics of DOC exported from permafrost catchments.

107 Given the high spatial heterogeneities of peatland and complexities of  
108 hydrological processes in permafrost regions, it is important to  
109 understand magnitudes and regulations on DOC export in different  
110 permafrost regions and especially in the south part of the Eurasian



111 continent where limited research has been performed. This study focuses  
112 on dynamics of DOC release from the Fukuqi River, a tributary of the  
113 Amur River positioned along northern slopes of the Great Xing'an  
114 Mountains in northeastern China. The Great Xing'an Mountains form an  
115 important barrier from Siberian cold air masses and monsoons of East  
116 Asia. The mean annual temperature of the area has on average increased  
117 by 0.3 °C every 10 years over the last 50 years, subjecting permafrost to  
118 higher risks of degradation. On the southern slopes of the Great Xing'an  
119 Mountains, the thickness of the active layer has increased by 20-40 cm  
120 from 1970s to 2000 (Jin et al., 2000). However, few studies have focused  
121 on possible effects of permafrost degradation on this region to date. This  
122 work thus investigates potential changes in DOC export patterns by  
123 answering the following questions:

124 (1) How much DOC is exported via stream discharge during the  
125 growing period?

126 (2) What is the relationship between runoff processes and  
127 concentrations, sources, and chemical characteristics of DOC?

128 (3) What are the potential effects of permafrost degradation and  
129 climate change?

130

## 131 **2. Approach and methodology**

### 132 **2.1. Study area**



133 Northern sections of the Great Xing'an Mountains in China are  
134 located along the southern margins of the continuous permafrost zone in  
135 Eurasia. The area represents the most remote region of the East Asia  
136 monsoon of the East Eurasian continent. The region includes  
137 approximately  $8.245 \times 10^3$  km<sup>2</sup> of natural wetland, representing a major  
138 proportion cold temperate wetlands and an important reservoir of soil  
139 carbon and usable water resources for northeastern China.

140 The Fukuqi River, a second order branch of the Amur River, is  
141 located at continuous permafrost zones of the northern section of the  
142 Great Xing'an Mountains (Fig. 1). The catchment extends across an area  
143 of 286.86 km<sup>2</sup> with an annual mean temperature of  $-4.2$  °C and a mean  
144 annual precipitation level of 425 mm (1959-2013). Large peatland areas  
145 have formed throughout the flat river valley. The peat layer, which is  
146 approximately 0.3-0.4 m thick, is composed of typical organic soil with  
147 organic matter levels ranging from 40% to 60% and with porosity levels  
148 ranging from 60% to 20% from the surface. According to previous field  
149 survey, the peatlands accounts for more than 90% of the total carbon  
150 stock in the catchment although it covers only about one-third of the total  
151 area. The maximum thaw depth of the active layer, ranging from 60 to 80  
152 cm, occurs usually in early August. Below the peat soil layer, there  
153 covers mineral soil with much lower organic content ( $< 5\%$ ) and soil  
154 porosity ( $< 10\%$ ) than the upper soil. The plants usually grow from May



155 until late September. The Sphagnum mosses (*S.capillifolium*, *S.*  
156 *magellanicum*) and sedges (*Eriophorum vaginatum*) are the dominant  
157 vegetation. The upland mountains on both sides of the valley are  
158 extensively covered by mineral soil and gravels with little organic  
159 content due to the continuous logging and frequent fires during the past  
160 60 years. To date, the original coniferous forest has been already replaced  
161 by yang *Pinus sylvestris var. mongolica*.

162

163 **Fig. 1** Geographic location of the study area.

164

## 165 **2.2. Sampling and monitoring program**

166 Monitoring was conducted from early May to late September of  
167 2012, 2013 and 2014. A gauging profile for DOC concentrations and  
168 hydrological parameters was set for the lower reaches of the Fukuqi  
169 River (Fig. 1). Water samples were collected from the stream profile  
170 every 1–5 days, and a higher sampling frequency was applied during  
171 flood periods while a lower sampling frequency was applied during low  
172 water periods. A 200 ml clean polyethylene bottle was used to obtain  
173 triplicate samples from the surface, middle, and bottom layers along the  
174 vertical direction of the profile. The collected water samples were filtered  
175 through a 0.45- $\mu\text{m}$  glass fibre membrane. Then, DOC concentrations in  
176 the samples were measured using a DOC analyser (C-VCPH, Shimadzu,





177 Japan) as soon as possible.

178         Meanwhile, the water level and mean flow velocity in the profile  
179 was automatically measured to evaluate stream discharge (Q) by a water  
180 level monitor (Odyssey, New Zealand, accuracy:  $\pm 2$  mm) and a flow  
181 meter (Argonaut-ADV, USA, accuracy:  $\pm 0.01$  m/s) respectively. Air  
182 temperature and soil temperature at 0–1.0 m depth were also recorded by  
183 an automatic microclimate gauging tower (Campbell, USA) set in the  
184 center part of the peatlands. The standing water levels were successively  
185 recorded by the same Odyssey monitor in the site nearby gauging tower.  
186 The thaw depth of the peatland active layer was manually surveyed  
187 weekly with a 1.0-m stainless steel ruler (accuracy: 0.1 cm) at the same  
188 three sites. Information of the temperature ( $^{\circ}\text{C}$ ), electrical conductivity  
189 (mS/cm), and turbidity (NTU) in the sampling profile is automatically  
190 obtained by a multi-parameter water quality sonde (YSI6600, USA). Part  
191 of the water quality data was lost in 2012 and 2013 due to the excessively  
192 low temperature in the stream.

193

194         To assess chemical DOC characteristics of the active layer and to  
195 determine sources of DOC in the discharge, peat soil pore water was  
196 collected from three sites located 50-100 m away from the main river  
197 channel in the growing seasons of 2013 and 2014 (Fig. 1). For each site,  
198 3-5 sample points were used repeatedly for each sampling procedure.



199 When sampling, 100 ml samples of soil pore water drawn from different  
200 depths at 10 cm intervals in the active layer were collected using ceramic  
201 soil pore water samplers (SIC20, Germany). Due to the gradual thawing  
202 of the active layer throughout the growing season, maximum sampling  
203 depths varied. Meanwhile, rainfall samples were during the two growing  
204 seasons. We ensured that the sample bottles did not contain any air in  
205 adherence with analysis requirements for stable oxygen isotopes ( $\delta^{18}\text{O}\text{‰}$ ).  
206 The depletion of stable oxygen isotopes ( $\delta^{18}\text{O}\text{‰}$ ) for the discharge  
207 samples, peat soil pore water and local rainfall in 2013 and 2014 were  
208 analysed with an isotope mass spectrometer (Finnigan Delta plus XP,  
209 USA) at the Key Laboratory of Wetland Ecology and Environment,  
210 Chinese Academy of Sciences.

211

### 212 **2.3. Fluorescence measurements**

213 Excitation-emission matrixes (EEMs) of the water samples were  
214 measured using a Hitachi F-7000 fluorescence spectrometer (Hitachi  
215 High Technologies, Japan) with a 50 W ozone-free Xenon arc lamp and  
216 R928P photomultiplier tube fitted as a detector. The spectrometer was set  
217 to collect signals using a 5-nm bandpass on excitation and emission  
218 monochromators at a scanning speed of 3,200 nm/min. EEMs were  
219 recorded for excitation spectra of between 220 and 400 nm and for  
220 emission spectra of between 300 and 500 nm. To eliminate the inner-filter



221 effect, samples were diluted with deionized water to a decadal UV  
222 absorbance at  $\lambda = 254$  nm of 0.2 absorbance units ( $\text{cm}^{-1}$ ). Milli-Q water  
223 blank EEMs were subtracted from the sample EEMs to eliminate Raman  
224 scatter peaks. Then, the EEMs were normalized to the area under the  
225 Raman scatter peak (excitation wavelength of 350 nm) of a Milli-Q water  
226 sample run the same day. The fluorescence intensities measured were  
227 reported in Raman Units (RU) in this study.

228 Three spectral indexes calculated from the EEMs were measured to  
229 quantify chemical characteristics of the dissolved organic matter: 1)  
230 humification (HIX) defined as the ratio of the sum of  $\lambda_{em} = 435\text{--}480$  nm  
231 to the sum of  $\lambda_{em} = 300\text{--}345$  for excitation at 254 nm and quantifying  
232 the complexity and aromaticity of dissolved organic matter. High HIX  
233 values denote the presence of highly humified or more complex organic  
234 matter (Ohno, 2002); 2) the fluorescence (FI) defined as the ratio of  
235 maximum emission fluorescence intensities at 450 and 500 nm for  
236 excitation at 370 nm identifies sources of humic-containing dissolved  
237 organic matter. The recommended FI for terrestrial-origin humics is 1.2  
238 and that for materials of microbial origin is 1.7 (Cory et al., 2010); 3) the  
239 biological index (BIX), defined as the ratio of intensities at  $\lambda_{em} 380$  nm  
240 and 430 nm for excitation at 310 nm, is a complementary index for  
241 evaluating the relative contributions of microbial-derived organic matter.  
242 BIX values of 1.0 or greater correspond to freshly produced DOC of



243 microbial origin, whereas values of 0.6 and lower imply the presence of  
244 little natural biological material (Huguet et al., 2009).

245

#### 246 **2.4. Statistical analyses**

247 The mean and the standard deviation of the DOC concentration in the  
248 stream and soil pore water, and the three fluorescence indices were  
249 statistically analyzed with the Statistical Program for Social Sciences  
250 (SPSS) version 13.0 software. The relationship between the hydrological  
251 factors and the DOC concentration and the fluorescence indices was  
252 examined by a two-tailed Pearson correlation and regression analysis,  
253 where the p-values were calculated to test for significance.

254

### 255 **3. Results**

#### 256 **3.1. Environmental conditions**

257 Substantial inter-annual and seasonal variations in precipitation were  
258 observed for the three years (Fig. 2). Total precipitation levels reached  
259 202.5, 520.8 and 164 mm in 2012, 2013 and 2014, respectively. Based on  
260 our statistics on the regional climate dataset for 1970 to 2005, 2013 was  
261 an extremely wet year due to excessive rainfall occurring in the spring  
262 and summer. Precipitation levels in the growing season of 2012 remained  
263 within a normal range while those for 2014 denote the presence of very  
264 dry conditions in the study area. Influenced by unusual precipitation



265 patterns, the mean air temperature of the growing season of 2013, 12.9°C,  
266 was somewhat lower than those of 2012 and 2014 (13.65 and 13.67°C).  
267 However, all mean values fell within the average range for the long-term  
268 climate dataset. We also found no significant differences in maximum  
269 thaw depths for the three years, finding values of approximately 70 cm.  
270 Standing water levels close to the stream channel declined overall across  
271 the growing seasons. No recorded data for higher than peat ground  
272 surface were detected for the three years.

273

274 **Fig. 2** Dynamics of air temperature, precipitation, standing water levels,  
275 and thaw depth observed during the growing seasons of 2012 to 2014.

276

### 277 **3.2. DOC concentrations and fluxes**

278 DOC concentrations in the Fukuqi River fluctuated considerably with  
279 discharge levels during the three growing seasons (Fig. 3). A maximum  
280 concentration of 44.71 mg L<sup>-1</sup> was found for the early spring of 2013  
281 accompanied by maximum flood levels for the three years. In the autumn,  
282 when flows were relatively low, DOC concentrations generally fell below  
283 8 mg L<sup>-1</sup>. It is worth noting that consistently high concentrations were  
284 recorded during two flood periods of the autumn of 2012 and of the  
285 spring of 2013. A significantly positive correlation was found between  
286 DOC concentrations and discharge levels for all three growing seasons



287 (n=92, p <0.01). Meanwhile, DOC concentrations were positively related  
288 to discharge turbidity and negatively related to discharge conductivity  
289 (n=68, p < 0.01) while no significant relationship was found between  
290 concentrations and air temperature or for soil temperatures of the active  
291 layer.

292 Mean DOC concentrations measured during the growing seasons  
293 were measured as 13.84, 19.98 and 13.82 mg/L for 2012, 2013 and 2014,  
294 respectively, with an overall mean value of 15.94 mg/L. Total DOC  
295 export magnitudes for the entire catchment were estimated as 1055.71,  
296 2467.37 and 672.59 t for the three respective years, denoting levels of  
297 DOC export of 3.68, 8.6 and 2.34 g m<sup>-2</sup>, respectively. Statistically  
298 speaking, the nine flood events (maximum discharge > 1.0 × 10<sup>6</sup> m<sup>3</sup> d<sup>-1</sup>)  
299 were responsible for 81% of the total DOC flux while the five floods  
300 with a discharge level of > 2.0 × 10<sup>6</sup> m<sup>3</sup> d<sup>-1</sup> accounted for 65% of the total  
301 flux. In total, approximately 85% of DOC was exported during flood  
302 periods.

303

304 **Fig. 3 Dynamics of dissolved organic carbon (DOC) concentrations and**  
305 **discharge observed during the growing seasons of 2012 to 2014. The**  
306 **discharge (Q) unit used is 10<sup>6</sup> m<sup>3</sup> d<sup>-1</sup>.**

307

308 **3.3. Spectral indexes of DOC**



309       The three spectral indexes varied considerably in terms of discharge  
310 processes during the growing seasons as is shown in Fig. 4. We found a  
311 positive correlation between the HIX and logarithmic discharge whereas  
312 both FI and BIX exhibited a significantly negative correlation with  
313 logarithmic discharge (Fig. 5). HIX ranged from 5.52 to 16.41 with an  
314 average value of 10.38, revealing a high volume of humification  
315 components in the stream discharge DOC (Ohno, 2002). This index and  
316 all of the other variables show significant relationships with hydrological  
317 DOC, Q, conductivity, and turbidity (Table 1). FI and BIX values ranged  
318 from 1.43 to 1.62 and from 0.46 to 0.63 with average values of 1.52 and  
319 0.54, respectively. The FI values indicate that DOC was derived from  
320 both terrestrial and microbial sources (Cory et al., 2010) while the BIX  
321 value denotes the presence of a low volume of fresh organic matter from  
322 biological sources in the runoff (Huguet et al., 2009). FI and BIX values  
323 were only closely related to hydrological variables; no relationship to  
324 temperature was found.

325

326 **Fig. 4 Relationships between discharge and the three spectral indexes**  
327 **during the growing seasons.**

328

329 **Fig. 5 Relationships between discharge and the three indexes during the**  
330 **study period.**



331

332 **Table 1. Correlation analysis of the three fluorescence indices with**  
333 **hydrological and climatic factors.**

334

### 335 **3.4. Stable oxygen isotopes in rivers, soil pore water, and rainfall**

336 We found nearly no seasonal variations in  $\delta^{18}\text{O}\text{‰}$  values from the  
337 rainfall and soil pore water samples (Fig. 6). It seems that air  
338 temperatures and rainfall quantities had no effect on the depletion of  
339 oxygen isotopes in rainfall during the growing seasons. The mean value  
340 of rainfall was measured at roughly  $-7.62 \pm 0.53\text{‰}$ , which is a  
341 significantly higher value than that found for river discharge and soil pore  
342 water ( $P < 0.01$ ). Two samples of river discharge collected in the early  
343 spring of 2013 clearly show higher values than those of the other samples,  
344 which fluctuated slightly around a mean value of roughly  $-14.64 \pm 0.87\text{‰}$   
345 during the other period. The  $\delta^{18}\text{O}\text{‰}$  values of soil pore water at the three  
346 sample sites did not vary by location or season. The mean value for the  
347 samples was recorded as  $-14.67 \pm 0.49\text{‰}$ , which is not statistical different  
348 from the value found for the river discharge samples ( $P < 0.01$ ).

349

350 **Fig. 6 Dynamics of stable oxygen isotope values for rainfall, discharge**  
351 **and soil pore water in the catchment.**

352





353 **3.5. DOC concentrations and fluorescence indexes of soil water**

354 During the growing seasons, DOC concentrations in the soil pore  
355 water changed considerably with depth. Maximum DOC concentrations  
356 were typically found in the plant root layer (36.98 mg L<sup>-1</sup>) while a  
357 minimum value of 15.36 mg L<sup>-1</sup> was found at the bottom of the profile  
358 (Fig. 7). DOC concentrations at different depths change to varying  
359 degrees during the growing seasons. However, we found no significant  
360 difference between average concentrations. There is a strong relationship  
361 between DOC concentrations and total soil organic matter, total nitrogen  
362 content levels and soil bulk density levels along the profile, and we found  
363 no relationships with soil temperature (Table 2). Similarly, no significant  
364 relationship was found between the average DOC concentration and the  
365 average soil temperature during the growing seasons.

366

367 **Fig. 7** DOC concentrations in soil pore water along the soil profile for  
368 2013.

369

370 **Table 2.** Results of the correlation analysis of dissolved organic carbon  
371 (DOC) in the soil pore water with soil factors

372

373 The HIX, FI, and BIX of the soil water samples varied greatly with  
374 soil depth (Figure 8). We found a pronounced change in the three indexes



375 at 30-40 cm, where we found soil organic matter levels to suddenly  
376 decline. HIX levels gradually decreased from the top to the bottom while  
377 FI and BIX levels were found to follow the opposite trend. For all of the  
378 collected samples, HIX levels were found to be significantly and  
379 positively related to DOC concentrations and to soil organic matter  
380 content levels ( $n = 18$ ,  $p < 0.01$ ) while FI and BIX levels were found to  
381 be inversely and significantly correlated with those parameters ( $n = 18$ ,  $p$   
382  $< 0.01$ ).

383

384 **Fig. 8 Vertical distribution of the three spectral indexes for soil pore**  
385 **water along the soil profile for 2013.**

386

## 387 **4. Discussion**

### 388 **4.1. Flow pathway and DOC concentrations**

389 DOC concentrations in permafrost catchments have been reported to  
390 vary considerably, and flow pathways are the most influential controllers  
391 of runoff events and entire growing seasons (Hagedorn et al., 2000;  
392 Dawson et al., 2008; Guo et al., 2015). Peatland in permafrost generally  
393 experiences subsurface flows but not over surface flows due to the  
394 occurrence of high levels of rainfall infiltration into the thawed organic  
395 layer (Carey and Woo, 1997). Resting on a frozen soil layer, infiltrated  
396 and previously stored water is prevented from draining deeper, and a



397 lateral subsurface flow parallel to the bottom of the active layer forms. It  
398 is worth noting that water previously stored close to the stream channel  
399 typically forms a major proportion of flood peaks owing to the high  
400 hydraulic conductivity of macroporous organic soil in peatland (Carey  
401 and Woo, 2001).

402 In the Fukuqi catchment, the porosity of peat in the upper 40 cm layer  
403 can generally reach levels of 20-60%. High infiltration rates and  
404 hydraulic conductivity levels found in the organic soil layer enable flow  
405 water to respond quickly to hydrological inputs and to transfer discharge  
406 into the channel. This prevents the formation of overland or surface flows.  
407 This serves as direct proof that the standing water level has never  
408 exceeded the peat surface and even during two large spring floods  
409 occurring in 2013. It is noteworthy that  $\delta^{18}\text{O}\text{‰}$  values in the discharge are  
410 generally similar to those in soil pore water close to the stream channel  
411 while being more negative than those in rainfall. This shows that the  
412 stream discharge is mainly composed of soil pore water reserved in the  
413 peatland area before new rainfall events occur, proving that lateral  
414 subsurface flows constitute the main form of runoff generation in the  
415 catchment.

416 Lateral subsurface flows are a fundamental condition of the positive  
417 relationship between runoff and DOC concentrations (Quinton and Gray,  
418 2003; Birkel et al., 2014; Guo et al., 2015). Subsurface flows guarantee



419 that the soil pore water reserved in peatlands before the rainfall event was  
420 pushed into the channel in order to the distance to the stream. The  
421 preferential output of peat water close to the channel characterized by  
422 high DOC concentrations contributes to a concentration peak occurring in  
423 flood periods and thus to a positive relationship between runoff and DOC  
424 concentrations during flooding periods, which lead to the same relation  
425 for runoff processes.

426

#### 427 **4.2. Hydrological connectivity and DOC export potential**

428 DOC exports from permafrost are also dependent on the connectivity  
429 of flow pathways that mobilize and transport DOC to streams (Köhler et  
430 al., 2002; Laudon et al., 2011). In permafrost catchments covered with  
431 peat-dominated soils, geomorphic landscape structures have been deemed  
432 crucial in determining the hydrological connectivity of peatland areas and  
433 upland hill slopes (Dawson et al., 2008). We found that peatland  
434 distributes along both sides of the stream channel as is shown in Fig. 1,  
435 revealing hydrological connectivity between the peatland area and stream  
436 during both flood and baseflow periods. It is noteworthy that the  
437 two-sided distribution of peatland prevents runoff flows from marginal  
438 hills from reaching the river channel directly despite entering the peatland  
439 area first (Guo et al., 2016). This is likely why  $\delta^{18}\text{O}\text{‰}$  values in the  
440 discharge samples are similar to those of the soil pore water while not



441 being affected by water volumes from upland hill slopes, for which  $\delta^{18}\text{O}\%$   
442 values should be similar to those of rainfall. Therefore, water volumes  
443 from upland areas, which contain low levels of DOC due to being  
444 covered with mineral soil and gravel, should not dilute DOC  
445 concentrations during floods. Simultaneously, permafrost across the  
446 whole catchment plays a central role by blocking the input path of  
447 shallow groundwater from upland areas. DOC concentrations during  
448 floods are only related to those of peat pore water. Hydrological  
449 connectivity maintained in the stream-peatland continuum centrally  
450 supports high DOC concentrations observed during floods.

451 It can therefore be speculated that exported DOC in the catchment is  
452 mainly “autochthonous” and derived from riparian peat throughout the  
453 growing season contrary to the recently accepted view that the source of  
454 DOC realised from headwater catchments is “allochthonous” from upland  
455 soils at least during wet seasons (Boyer et al., 1996; Inamdar et al., 2006;  
456 Sanderman et al., 2009). In fact, “autochthonous” DOC export results not  
457 only from the simple landscape structure of the stream-peatland-upland  
458 continuum along the catchment transect but also from the high DOC  
459 production capacities of peatland. Though we did not conduct direct  
460 experiments on this issue, the field data show high levels of DOC  
461 production potential for peatland in the catchment. According to our data  
462 on soil pore water, DOC concentrations in the peat pore water have



463 always been high across seasons and were accompanied by several large  
464 floods in 2013 (Fig. 7). Importantly, DOC concentrations in the discharge  
465 show no clear drawdown during two successive flooding periods in the  
466 spring (Fig. 3), revealing the weak influence of successive exports of  
467 floodwater on DOC concentrations in soil pore water. As a balance  
468 between DOC production and dissolution can re-occur within hours under  
469 suitable conditions (Worrall et al., 2008), the DOC production rate is not  
470 the limiting factor that controls export concentrations.

471

#### 472 **4.3. DOC sources and chemical characteristics**

473 Carey and Woo (2001) describe permafrost soil in reference to a  
474 two-layer flow system based on the difference in hydraulic conductivity  
475 between the upper organic soil layer and lower mineral soil layer. As  
476 hydraulic conductivity levels typically decline exponentially in the  
477 transition from organic to mineral soil, DOC levels in discharge during  
478 the flood period derive mostly from the upper organic layer while DOC  
479 levels of the recession and baseflow periods are mainly derived from the  
480 lower mineral soil layer in the study catchment (Guo et al., 2015).  
481 Therefore, considerable variations in DOC chemical compositions along  
482 the vertical soil profile are bound to affect their performance in the  
483 discharge examined in this study. The three fluorescence indexes of HIX,  
484 FI, and BIX, which generally show no changes for diluted DOC



485 concentrations, serve as robust indicators of sources of stream discharge.  
486 Considerable variations in the three indexes observed during flood events  
487 prove the occurrence of changes in DOC sources following a shift from  
488 the flood to the baseflow phase. Flood DOC, which is characterized by  
489 higher levels of humification and by the presence of few  
490 microbial-originated organic components, can be identified from the  
491 upper soil layer of the peatland area while DOC in the baseflow is  
492 derived from the lower mineral soil layer. Previous studies of permafrost  
493 catchments have recorded shifts in DOC compositions attributed to  
494 different source water contributions across seasons (Spencer et al., 2008;  
495 O'Donnell et al., 2010). However, our results highlight shifts in DOC  
496 chemistry through rainfall-runoff processes. Lambert et al. (2014) have  
497 also confirmed the presence of a shift in DOC sources between riparian  
498 wetland areas and upland areas during flood events in a DOC-limited  
499 upland catchment, revealing the unpredictable complexity of DOC source  
500 during floods due to effects of landscape structures, hydrological  
501 pathways, and organic carbon mineralization patterns. From our study  
502 results, it is easy to understand that the shift in water sources from the  
503 upper soil layer to the lower soil layer during flooding can be attributed to  
504 great discrepancies in hydraulic conductivity observed in the autumn  
505 once the lower mineral soil layer has thawed. However, such shifts are  
506 also clearly observed in the spring when the upper soil is still frozen (Fig.



507 2 and 4). This suggests the presence of another DOC source such as litter  
508 covering the peatland area in the spring, which could easily release DOC  
509 from rainfall extraction. Thus, a more detailed survey of litter- and  
510 upland-originated DOC is urgently needed in future research.

511 The deepening of the soil active layer will alter the discharge flow  
512 pathway and in turn DOC sources and chemical characteristics. As few  
513 rainfall events occurred in 2014, we were able to identify effects of the  
514 gradual deepening of the active layer throughout growing seasons. We  
515 find a remarkable elevation in BIX and FI levels in discharge from the  
516 spring to the autumn when flood periods are disregarded (Fig. 4),  
517 highlighting the influence of active layer depths on DOC sources and  
518 chemical characteristics. The elevations found suggest that an increase in  
519 microbial-originated DOC from the lower soil layer increases discharge  
520 levels following the deepening of the soil active layer. This result is  
521 consist with the conclusions of Prokushkin et al. (2007) who also found  
522 higher levels of microbially transformed and/or derived material export  
523 due to the presence of a deeper active layer in the summer and autumn in  
524 Siberia. Changes in biochemical compositions (decreases in the  
525 lignocellulose complex; increases in the hydrophilic fraction) are  
526 confirmed further in Kawahigashi et al. (2004).

527 From our results, the humification degree of DOC as determined by  
528 HIX shows no clear trend for the seasons of 2014. HIX values fluctuate





529 considerably even following a minor flood, showing that the hydrological  
530 process considerably controls the humification of exported DOC. As is  
531 shown in Fig. 8, HIX values in the deeper soil layer change little from  
532 June to August while BIX and FI values do not, and this likely spurred  
533 the differing performance of the three indexes in terms of stream  
534 discharge levels during the seasons of 2014. It can be concluded that FI  
535 and BIX values are both sensitive to flooding processes and soil active  
536 layer depths while HIX values only respond to flooding processes.  
537 Therefore, the three indexes respond differently to different  
538 environmental factors, and a joint analysis will help reveal the chemical  
539 characteristics of organic matter synthetically.

540

#### 541 **4.4. Export magnitude and potential**

542 Several characteristics of permafrost peatland (e.g., high organic  
543 matter content levels, low water temperatures, weak microbial  
544 transformations, and high levels of hydraulic transmission) result in large  
545 magnitudes and in strong potential for DOC export (Balcarczyl, et al.,  
546 2009; Lessels et al., 2015). According to our data, levels of net DOC  
547 export from the studied catchment are estimated at  $4.87 \text{ g m}^{-2} \text{ yr}^{-1}$ , which  
548 is in the lower range of reported permafrost estimates ranging from 1 to  
549  $35 \text{ g C m}^{-1} \text{ yr}^{-1}$  (Fraser et al., 2001; Dinsmore et al., 2010). Roughly  
550 two-thirds of the catchment is covered in mountain gravel and mineral



551 soil with low levels of organic carbon in the Fukuqi catchment, likely  
552 decreasing the mean DOC export capacity of the whole catchment.  
553 According to our field survey, carbon stock in the peatland area accounts  
554 for approximately 90% of carbon levels in the catchment (Miao, 2014).  
555 Assuming that the DOC originates from both peatland and forests and  
556 that the total export level is proportional to the organic carbon pool in the  
557 soil of each ecosystem, DOC exported from the peatland area can be  
558 estimated at  $12.89 \text{ g m}^{-2} \text{ yr}^{-1}$  on average. According to Miao (2014), the  
559 net ecosystem exchange (NEE) of peatland in the study catchment  
560 determined from carbon dioxide and methane fluxes between peatland  
561 surfaces and the atmosphere is  $30.59 \pm 1.98 \text{ g C m}^{-2} \text{ yr}^{-1}$ . Therefore, the  
562 DOC export magnitude should account for 72.8% of the NEE of the  
563 peatland area, as the verified NEE was calculated as  $17.7 \text{ g C m}^{-2} \text{ yr}^{-1}$   
564 ( $30.59-12.89$ ). Theoretically, the data are overestimated due to our  
565 assumption of a linear relationship between carbon storage and DOC  
566 export magnitudes. However, our data still highlight the importance of  
567 stream carbon export for peatland net ecosystem carbon balance. Any  
568 disturbance altering DOC export magnitudes should disrupt the balance  
569 between of carbon sequestration and release in the peatland area.

570 The results highlight that DOC export magnitudes from the  
571 permafrost catchment depend mainly on the discharge volume at the time  
572 scale for the whole seasonal period. As noted above, our results prove that



573 DOC export concentrations vary considerably based on discharges of the  
574 observed magnitude and frequencies of the three years while DOC  
575 concentrations in the peatland area remain relatively stable across the  
576 seasons. This finding is consistent with previous work suggesting that the  
577 DOC export from permafrost organic soils is rainfall- and not  
578 carbon-limited (Judd and Kling, 2002; Prokushkin et al. 2008; Olfeldt and  
579 Roulet, 2012). Therefore, total rainfall levels are a robust predictor of  
580 future pathways of DOC export from the catchment. It has been predicted  
581 that precipitation in the study area will increase by 15.95% at most over  
582 the next 50 years based on observational data on CN05 and based on the  
583 outputs of 26 CMIP5 (Coupled Model Inter-comparison Project Phase 5)  
584 models (Tao et al., 2016). Hence, the DOC export magnitude from the  
585 permafrost is likely to increase following precipitation, which should  
586 greatly enhance risks of losing an important active carbon pool in the  
587 northern region of the Great Xing'an Mountains. As few data have been  
588 generated of the southern margins of Eurasian permafrost to date, more  
589 detailed investigations and data on the region are urgently needed to  
590 evaluate future land carbon responses to climate change.

591

## 592 **5. Conclusions**

593 Eurasian permafrost serves as an important potential carbon pool for  
594 the atmosphere and for linked aquatic and ocean ecosystems.



595 Investigations of DOC responses to permafrost peatland can be used to  
596 predict the ecological consequences of climatic change in these regions.  
597 Our study thoroughly explains the characteristics and determinants of  
598 DOC export from a peatland catchment along the southern margins of  
599 Eurasian permafrost. DOC magnitudes, sources, and chemical  
600 characteristics in stream discharge are greatly affected by runoff  
601 processes. Stable oxygen isotopes show that flood volumes and DOC  
602 exported in flood periods mainly derive from peat pore water stored in the  
603 upper organic layer of the soil profile prior to rainfall events. DOC  
604 concentrations are significantly related to stream discharge levels due to  
605 strong levels of hydrological connectivity between peatland areas and  
606 streams, thus rendering stream discharge (and flood volumes in particular)  
607 a strong indicator of DOC export magnitude. The three fluorescence  
608 indexes of HIX, FI and BIX show that DOC source and chemical  
609 characteristics change considerably with discharge processes. A  
610 deepening of active layer following permafrost degradation should  
611 increase levels of microbial-originated DOC content in baseflow  
612 discharge by elevating DOC contribution from the lower mineral soil  
613 layer. From our field data, the catchment exhibits strong potential for  
614 annual DOC export ( $4.87 \text{ g C/m}^2$ ), and DOC levels for the peatland  
615 landscape are estimated at  $12.89 \text{ g C/m}^2$ , representing 72.8% of the net  
616 ecosystem exchange (NEE). Given the potential for increases in



617 precipitation in the study region, DOC export levels are expected to  
618 increase in the future, accelerating the loss of dissolved carbon pools  
619 from East Asian permafrost.

620

### 621 **Acknowledgements**

622 The work was supported by National Key Research and Development  
623 Program of China (2016YFA0602303), National Natural Science  
624 Foundation of China (41571097), Key of Frontier Sciences, Chinese  
625 Academy of Sciences (QYZDJ-SSW-DQC013), Research Program of  
626 Northeast Institute of Geography and Agroecology, Chinese Academy of  
627 Science (IGA-135-05).

628

### 629 **References**

630 Ågren, A., Haei, M., Köhler, S. J., Bishop, K., Laudon, H.: Regulation of  
631 stream water dissolved organic carbon (DOC) concentrations during  
632 snowmelt; the role of discharge, winter climate and memory effects,  
633 *Biogeosciences*, 7, 2901–2913, 2010.

634 Balcarczyk, K.L., Jones Jr, J.B., Jaffé, R., Maie, N.: Stream dissolved  
635 organic matter bioavailability and composition in watersheds  
636 underlain with discontinuous permafrost, *Biogeochemistry*, 94, 255–  
637 270, 2009.

638 Birkel, C., Soulsby, C., Tetzlaff, D.: Integrating parsimonious models of



- 639 hydrological connectivity and soil biogeochemistry to simulate stream  
640 DOC dynamics, *J. Geophys. Res. Biogeosci.*, 119, 1030 – 1047, 2014.
- 641 Boyer, E. W., Hornberger, G. M., Bencala, K. E., and McKnight, D. M.:  
642 Overview of a simple model describing variation of dissolved organic  
643 carbon in an upland catchment, *Ecol. Modell.*, 86, 183–188, 1996.
- 644 Carey, S., Woo, M.K.: Snowmelt hydrology of two subarctic slopes,  
645 Southern Yukon, Canada. In *Proceedings of the Eleventh Northern  
646 Research Basins Symposium and Workshop (Vol 2)*, Prudhoe  
647 Bay/Fairbanks Alaska. The Water and Environmental Research  
648 Centre, University of Alaska, Fairbanks, pp. 15–35, 1997.
- 649 Carey, S.K., Woo, M.K.: Slope runoff processes and flow generation in a  
650 subarctic, subalpine catchment, *J. Hydrol.*, 253, 110–129, 2001.
- 651 Cory, R.M., Miller, M.P., McKnight, D.M., Guerard, J.J., Miller, P.L.:  
652 Effect of instrument-specific response on the analysis of fulvic acid  
653 fluorescence spectra. *Limnology and Oceanography: Methods* 8: 67–  
654 78, 2010.
- 655 Cory, R.M., Ward, C.P., Crump, B.C., Kling, G.W.: Sunlight controls  
656 water column processing of carbon in arctic fresh waters, *Science*,  
657 345, 925–928, 2014.
- 658 Dawson, J.J.C., Soulsby, C., Tetzlaff, D., Hrachowitz, M., Dunn, S.M.,  
659 Malcolm, I.A.: Influence of hydrology and seasonality on DOC  
660 exports from three contrasting upland catchments. *Biogeochemistry*,



- 661 90, 93–113, 2008.
- 662 Dinsmore, K.J., Billett, M.F., Skiba, U.M., Rees, R.M., Drewer, J.,  
663 Helfter, C.: Role of the aquatic pathway in the carbon and greenhouse  
664 gas budgets of a peatland catchment, *Global Change Biol.*, 16, 2750–  
665 2762, 2010.
- 666 Frey, K. E., McClelland, J. W.: Impacts of permafrost degradation on  
667 arctic river biogeochemistry, *Hydrol. Process.*, 23, 169–182, 2009.
- 668 Fraser, C.J.D., Roulet, N.T., Moore, T.R.: Hydrology and dissolved  
669 organic carbon biogeochemistry in an ombrotrophic bog, *Hydrol.*  
670 *Process.*, 15, 3151–3166, 2001.
- 671 Guo, Y.D., Song, C.C., Wan, Z.M., Lu, Y.Z., Qiao, T.H., Tan, W.W.,  
672 Wang, L.L.: Dynamics of dissolved organic carbon release from a  
673 permafrost wetland catchment in northeast China. *J. Hydrol.*, 531,  
674 919–928, 2015.
- 675 Guo, Y.D., Song, C.C., Wang, L.L., Tan, W.W., Wang, X.W., Cui, Q.,  
676 Wan, Z.M.: Concentrations, sources, and export of dissolved CH<sub>4</sub> and  
677 CO<sub>2</sub> in rivers of the permafrost wetlands, northeast China, *Ecol. Eng.*,  
678 90, 491–497, 2016.
- 679 Hagedorn, F., P. Schleppei, P. Waldner, and H. Flühler.: Export of  
680 dissolved organic carbon and nitrogen from Gleysol dominated  
681 catchments: The significance of water flow paths. *Biogeochemistry*,  
682 50, 137–161, 2000.



- 683 Holden, J.: Peatland hydrology and carbon release: why small-scale  
684 process matters, *Philos. T. Roy. Soc. A.*, 363, 2891–2913, 2005.
- 685 Huguet, A., Vacher, L., Relexans, S., Saubusse, S., Froidefond, J.M.,  
686 Parlanti, E.: Properties of fluorescent dissolved organic matter in the  
687 Gironde Estuary, *Org. Geochem.*, 40, 706–719, 2009.
- 688 Inamdar, S. P. and Mitchel, M. J.: Hydrologic and topographic controls  
689 on storm-event exports of dissolved organic carbon (DOC) and nitrate  
690 across catchment scales, *Water Resour. Res.*, 42, W03421,  
691 doi:10.1029/2005WR004212, 2006.
- 692 Jin, H.J., Li, S.X., Cheng, G.D., Wang, S.L., Li, X.: Permafrost and  
693 climatic change in China, *Global Planet., Change* 26, 387–404, 2000.
- 694 Judd, K.E., Kling, G.W.: Production and export of dissolved C in arctic  
695 tundra mesocosms: the roles of vegetation and water flow,  
696 *Biogeochemistry*, 60, 213–234, 2002.
- 697 Kalbitz, K., Schwesig, D., Rethemeyer, J., Matzner, E.: Stabilization of  
698 dissolved organic matter by sorption to the mineral soil, *Soil Biol*  
699 *Biochem.*, 37, 1319–1331, 2005.
- 700 Kawahigashi, M., Kaiser, K., Kalbitz, K., Rodionov, A., Guggenberger,  
701 G.: Dissolved organic matter in small streams along a gradient from  
702 discontinuous to continuous permafrost, *Global Change Biol.*, 10,  
703 1576–1586, 2004.
- 704 Kicklighter, D. W., Hayes, D. J., McClelland, J. W., Peterson, B. J.,





- 705 McGuire, A. D., Melillo, J. M.: Insights and issues with simulating  
706 terrestrial DOC loading of Arctic river networks, *Ecol. Appl.*, 23,  
707 1817–1836, 2013.
- 708 Köhler, S. J., Buffam, I., Jonsson, A., Bishop, K.H.: Photochemical and  
709 microbial processing of stream and soil water dissolved organic  
710 matter in a boreal forested catchment in northern Sweden, *Aquat. Sci.*,  
711 64, 269–81, 2002.
- 712 Lambert, T., Pierson-Wickmann, A.C., Gruau, G., Jaffrezic, A., Petitjean,  
713 P., Thibault, J. N., Jeanneau, L.: DOC sources and DOC transport  
714 pathways in a small headwater catchment as revealed by carbon  
715 isotope fluctuation during storm events, *Biogeosciences*, 11, 3043–  
716 3056, 2014.
- 717 Laudon, H., Berggren, M., Ågren, A., Buffam, I., Bishop, K., Grabs, T.,  
718 Jansson, M., Köhler, S.: Patterns and dynamics of dissolved organic  
719 carbon (DOC) in boreal streams: the role of processes, connectivity,  
720 and scaling, *Ecosystems*, 14, 880–893, 2011.
- 721 Lessels, J.S., Tetzlaff, D., Carey, S.K., Smith, P., Soulsby, C.: A coupled  
722 hydrology-biogeochemistry model to simulate dissolved carbon  
723 exports from a permafrost-influenced catchment. *Hydro. Process.*, 29,  
724 5383–5396, 2015.
- 725 Lyon, S. W., Destouni, G., Giesler, R., Humborg, C., Mörth, M., Seibert,  
726 J., Karlsson, J., and Troch, P. A.: Estimation of permafrost thawing



- 727 rates in a sub-arctic catchment using recession flow analysis, Hydrol.  
728 Earth Syst. Sci., 13, 595–604, 2009.
- 729 Lyon, S.W., Morth, M., Humborg, C., Giesler, R., Destouni, G.: The  
730 relationship between subsurface hydrology and dissolved carbon  
731 fluxes for a sub-arctic catchment, Hydrol. Earth Syst. Sci., 14, 941–  
732 950, 2010.
- 733 Mann, P.J., Davydova, A., Zimov, N., Spence, R.G.M., Davydov, S.,  
734 Bulygina, E., Zimov, S., Holmes, R.M.: Controls on the composition  
735 and lability of dissolved organic matter in Siberia’s Kolyma river  
736 basin, J. Geophys. Res.-Biogeo., 117, G01028. DOI:  
737 10.1029/2011JG001798, 2012.
- 738 Miao, Y.Q.: Net ecosystem carbon fluxes of peatland in the continuous  
739 permafrost zone, Great Hinggan Mountains. Dissertation. University  
740 of Chinese Academy of Sciences. pp, 120, 2014. (in Chinese)
- 741 Ohno, T.: Fluorescence inner-filtering correction for determining the  
742 humification index of dissolved organic matter, Environ. Sci.  
743 Technol., 36, 742–746, 2002.
- 744 O’Donnell, J. A., Aiken, G. R., Kane, E. S., Jones, J. B.: Source water  
745 controls on the character and origin of dissolved organic matter in  
746 streams of the Yukon River basin, Alaska, J. Geophys. Res., 115,  
747 G03025, doi:10.1029/2009JG001153, 2010.
- 748 Olefeldt, D., Roulet, N.T.: Effects of permafrost and hydrology on the



- 749 composition and transport of dissolved organic carbon in a subarctic  
750 peatland complex, *J. Geophys. Res.*, 117, G01005,  
751 doi:10.1029/2011JG001819, 2012.
- 752 Olefeldt, D., Roulet, N.T.: Permafrost conditions in peatlands regulate  
753 magnitude, timing, and chemical composition of catchment dissolved  
754 organic carbon export, *Global Change Biol.*, 20, 3122–3136, 2014.
- 755 Opsahl, S., Benner R., Amon R. M. W.: Major flux of terrigenous  
756 dissolved organic matter through the Arctic Ocean, *Limnol.*  
757 *Oceanogr.*, 44, 2017–2023, 1999.
- 758 Petrone, K.C., Jones, J.B., Hinzman, L.D., Boone, R.D.: Seasonal export  
759 of carbon, nitrogen, and major solutes from Alaskan catchments with  
760 discontinuous permafrost, *J. Geophys. Res.*, 111, G02020,  
761 doi:10.1029/2005JG000055, 2006.
- 762 Prokushkin, A.S., Tokareva, I.V., Prokushkin, S.G., Abaimov, A.P.,  
763 Guggenberger, G.: Fluxes of dissolved organic matter in larch forests  
764 in the Cryolithozone of Siberia, *Russ. J. Ecol.* 2, 39, 151–159, 2008.
- 765 Prokushkin, A.S., Gleixner, G., McDowell, W.H., Ruehlow, S., Schulze,  
766 E.D.: Source and substrate-specific export of dissolved organic matter  
767 from permafrost-dominated forested watershed in central Siberia,  
768 *Global Biogeochem. Cy.*, 103, 109–124, 2007.
- 769 Quinton, W.L., Gray, D.M.: Subsurface Drainage from Organic Soils in  
770 Permafrost Terrain: The Major Factors to be Represented in a Runoff



- 771 Model, 8th International Conference on Permafrost, Permafrost, Vols  
772 1 AND 2, 917–922, 2003.
- 773 Sanderman, J., Lohse, K. A., Baldock, J. A., and Amundson, R.: Linking  
774 soils and streams: sources and chemistry of dissolved organic matter  
775 in a small coastal watershed, *Water Resour. Res.*, 45, W03418,  
776 doi:10.129/2008WR006977, 2009.
- 777 Spencer, R. G. M., Aiken, G. R., Wickland, K. P., Striegl, R. G., Hernes,  
778 P. J.: Seasonal and spatial variability in dissolved organic matter  
779 quantity and composition from the Yukon River basin, Alaska, *Global*  
780 *Biogeochem. Cycles*, 22, GB4002, doi:10.1029/2008GB003231,  
781 2008.
- 782 Striegl, R.G., Aiken, G.R., Dornblaser, M.M., Raymond, P.A., Wickland,  
783 K.P.: A decrease in discharge-normalized DOC export by the Yukon  
784 River during summer through autumn, *Geophys. Res. Lett.*, 32,  
785 L21413. DOI:10.1029/2005GL024413, 2005.
- 786 Striegl, R.G., Dornblaser, M.M., Aiken, G.R., Wickland, K.P., Raymond,  
787 P.A.: Carbon export and cycling by the Yukon, Tanana, and  
788 Porcupine rivers, Alaska 2001–2005, *Water Resour. Res.*, 43,  
789 W02411, doi:10.1029/2006WR00, 2007.
- 790 Tao, C.W., Jiang, C., Sun, J.X.: Projection of future changes in climate in  
791 Northeast China using a CMIP5 multi-model ensemble, *Chinese J.*  
792 *Geophys-CH.*, 59, 3580–3591, 2016.



793 Townsend-Small, A., McClelland, J.W., Max Holmes, R., Peterson, B. J.:

794 Seasonal and hydrologic drivers of dissolved organic matter and

795 nutrients in the upper Kuparuk River, Alaskan Arctic,

796 Biogeochemistry, 103,109–124, 2011.

797 Vonk, J. E., Mann, P. J., Davydov, S., Davydova, A., Spencer, R. G. M.,

798 Schade, J., Sobczak, W. V., Zimov, N., Zimov, S., Bulygina, E.,

799 Eglinton, T. I.: High biolability of ancient permafrost carbon upon

800 thaw, Geophys. Res. Lett., 40, 2689–2693, 2013.

801 Worrall, F., Gibson, H.S., Burt T.P.: Production vs. solubility in

802 controlling runoff of DOC from peat soils – The use of an event

803 analysis, J. Hydrol., 358, 84– 95, 2008.

804

805

806

807

808

809

810

811

812

813

814



815

816

817 **Table 1.** Correlation analysis of the three fluorescence indices with hydrological and  
 818 climatic factors.

		DOC	Q	Conductivity	Turbidity	T <sub>air</sub>	T <sub>soil</sub>
HIX	Pearson	0.708**	0.609*	0.451**	-0.592**	0.342	0.395*
	Sig. (2-tailed)	0.000	0.000	0.005	0.000	0.115	0.02
	n	92	92	68	68	92	92
FI	Pearson	-0.594**	-0.606**	-0.477**	0.469**	0.353	0.389
	Sig. (2-tailed)	0.000	0.000	0.004	0.001	0.203	0.128
	n	92	92	68	68	92	92
BIX	Pearson	-0.64**	-0.707**	-0.488**	0.322*	-0.027	0.384
	Sig. (2-tailed)	0.001	0.000	0.001	0.012	0.823	0.129
	n	92	92	68	68	92	92

819 DOC is dissolved organic carbon; Q is stream discharge; T<sub>air</sub> is the average air  
 820 temperature over the past three days; T<sub>soil</sub> is the average soil temperature of the active  
 821 layer; “\*\*” denotes p < 0.01; “\*” denotes p < 0.05

822

823

824

825

826

827 **Table 2.** Results of the correlation analysis of dissolved organic carbon (DOC) in the  
 828 soil pore water with soil factors

		SOM	TN	TP	Bulk density	Water content	T <sub>soil</sub>
DOC	Pearson	0.733**	0.602*	0.341	-0.671**	0.337	0.492
	Sig. (2-tailed)	0.000	0.02	0.187	0.005	0.144	0.07
	n	18	18	18	18	18	18

829 SOM, TN and TP denote soil organic matter content, total nitrogen and phosphorus respectively;

830 T<sub>soil</sub> is the soil mean temperature at each depth; “\*\*” denotes p < 0.01; “\*” denotes p < 0.05.

831



832  
833  
834  
835  
836  
837  
838  
839  
840  
841  
842  
843  
844  
845  
846  
847  
848  
849  
850  
851  
852  
853  
854  
855  
856  
857  
858  
859  
860  
861  
862  
863  
864  
865  
866  
867  
868  
869  
870  
871  
872  
873  
874  
875

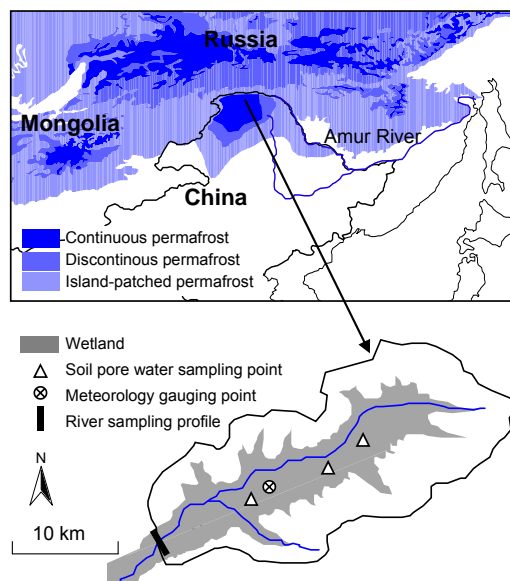
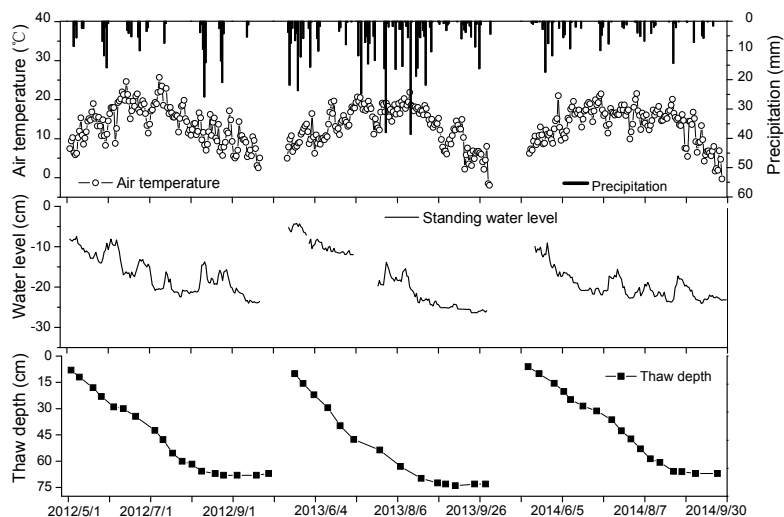


**Fig. 1** Geographic location of the study area



876  
877  
878  
879  
880  
881  
882  
883  
884  
885  
886  
887  
888  
889  
890  
891  
892  
893  
894  
895



896 **Fig. 2** Dynamics of air temperature, precipitation, standing water levels, and thaw  
897 depth observed during the growing seasons of 2012 to 2014.

898  
899  
900  
901  
902  
903  
904  
905  
906  
907  
908  
909  
910  
911





912

913

914

915

916

917

918

919

920

921

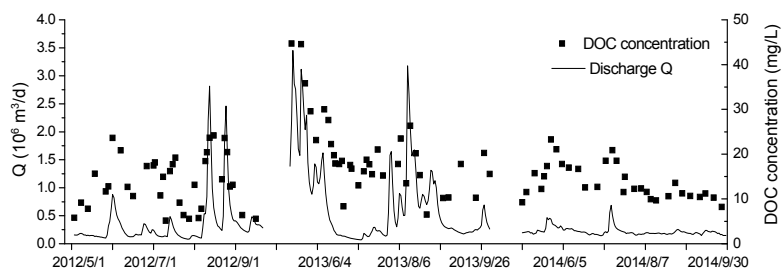
922

923

924

925

926



927

928 **Fig. 3** Dynamics of dissolved organic carbon (DOC) concentrations and discharge  
929 observed during the growing seasons of 2012 to 2014. The discharge (Q) unit used is  
930  $10^6 \text{ m}^3 \text{ d}^{-1}$ .

931

932

933

934

935

936

937

938

939

940

941

942

943

944

945

946



947

948

949

950

951

952

953

954

955

956

957

958

959

960

961

962

963

964

965

966

967

968

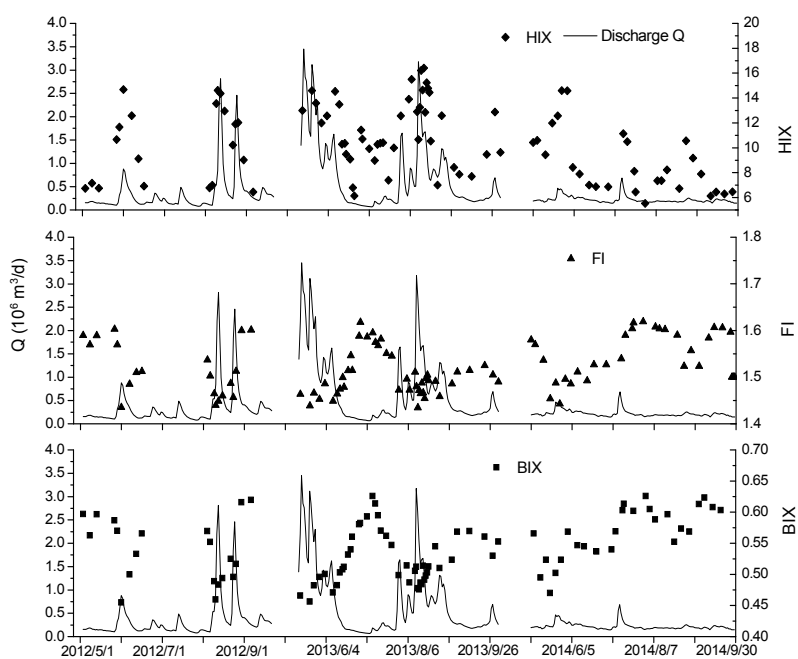
969

970

971

972

973



974

974 **Fig. 4** Relationships between discharge and the three spectral indexes during the  
975 growing seasons.

976

977

978

979

980

981

982

983

984



985

986

987

988

989

990

991

992

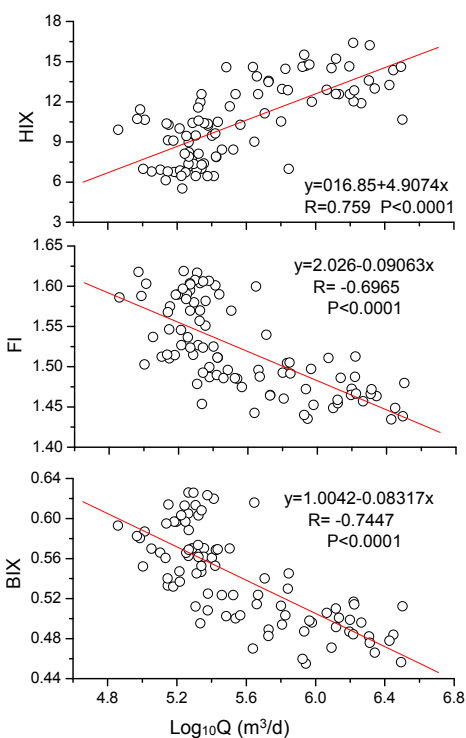
993

994

995

996

997



998

999

1000

1001

1002

1003

1004

1005

1006

1007

1008

1009

1010

1011

1012

1013

1014

1015

**Fig. 5** Relationships between discharge and the three indexes during the study period.

1016

1017

1018

1019

1020

1021

1022

1023



1024

1025

1026

1027

1028

1029

1030

1031

1032

1033

1034

1035

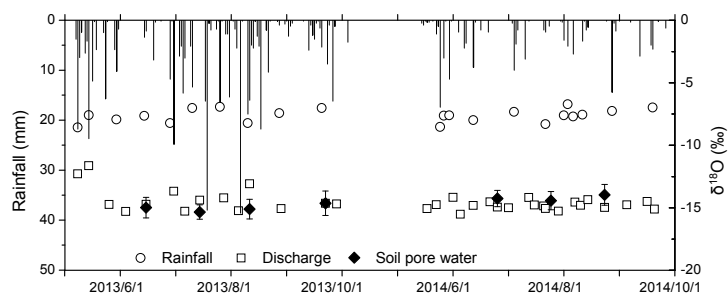
1036

1037

1038

1039

1040



1041

**Fig. 6** Dynamics of stable isotope oxygen values for rainfalls, discharge and soil pore water in the catchment.

1043

1044

1045

1046

1047

1048

1049

1050

1051

1052

1053

1054

1055



1056  
1057  
1058  
1059  
1060  
1061  
1062  
1063  
1064  
1065  
1066  
1067  
1068  
1069  
1070  
1071  
1072  
1073  
1074  
1075  
1076  
1077  
1078  
1079  
1080  
1081  
1082  
1083  
1084  
1085  
1086  
1087  
1088  
1089  
1090  
1091  
1092  
1093  
1094  
1095  
1096  
1097  
1098

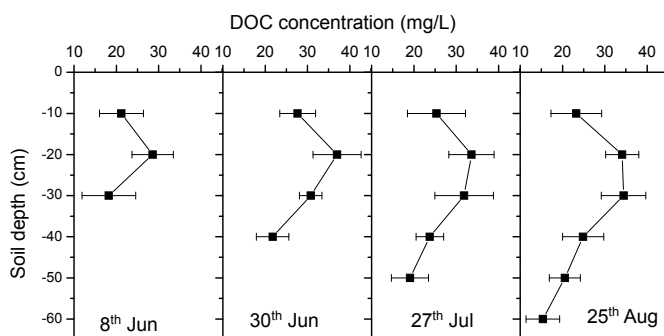


**Fig. 7** DOC concentrations in soil pore water along the soil profile for 2013.



1099  
1100  
1101  
1102  
1103  
1104  
1105  
1106  
1107  
1108  
1109  
1110  
1111  
1112  
1113  
1114  
1115  
1116  
1117  
1118  
1119  
1120  
1121  
1122  
1123  
1124  
1125  
1126  
1127  
1128  
1129  
1130  
1131  
1132  
1133

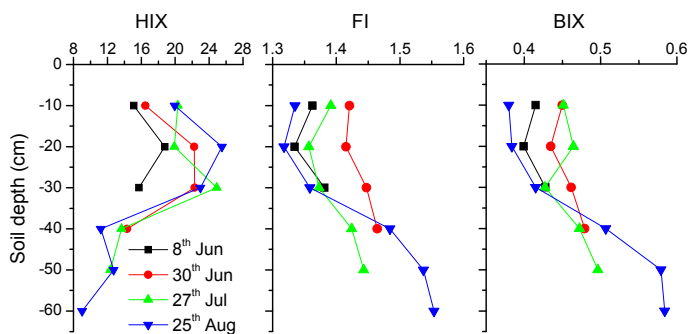


**Fig. 8** Vertical distribution of the three spectral indexes for soil pore water along the soil profile for 2013.